Use of directly molded poly(methyl methacrylate) channels for microfluidic applications

Sung Hoon Lee,†[a] Do Hyun Kang,†[a] Hong Nam Kim[a] and Kahp Y. Suh*[ab]

Received 18th June 2010, Accepted 18th August 2010
DOI: 10.1039/c0lc00127a

A direct molding method for creating a homogeneous, polymer microfluidic channel is presented. By utilizing capillary rise and subsequent absorption of poly(methyl methacrylate) (PMMA) solution into a solvent-permeable poly(dimethyl siloxane) (PDMS) mold, various circular or elliptic polymer microchannels were fabricated without channel bonding and additional surface modification processes. In addition, the channel diameter was tunable from several micrometres to several hundreds of micrometres by controlling concentration and initial amount of polymer solution for a given PDMS mold geometry. The molded PMMA channels were used for two applications: blocking absorption of Rhodamine B dye and constructing artificial endothelial cell-cultured capillaries. It was observed that the molded PMMA channels effectively prevented absorption and diffusion of Rhodamine molecules over 5 h time span, demonstrating approximately 40 times higher blocking efficiency as compared to porous PDMS channels. Also, calf pulmonary artery endothelial cells (CPAEs) adhered, spread, and proliferated uniformly within the molded microchannels to form near confluency within 3 days and remained viable at day 6 without notable cell death, suggesting high biocompatibility and possibility for emulating *in vivo*-like three-dimensional architecture of blood vessels.

Introduction

Polymer-based microfluidic systems are being increasingly used in the fields of hydrodynamics, bioassays, and tissue engineering, due to their various attractive features such as low cost, mechanical flexibility, and biocompatibility.[1–3] To be more amenable for microfluidic applications, construction of a polymer microchannel in a rapid and inexpensive manner is one of the key prerequisites, together with other requirements including optical transparency, chemical compatibility, and system integration.[4,5]

To date, a variety of strategies have been introduced to fabricate polymer microchannels, involving rapid prototyping,[6] photopolymerization,[7] liquid molding,[8] cracking,[9] wrinkling,[10] parylene bonding/micromolding,[11] and UV-assisted sealing.[12] Although these approaches offer useful tools to the construction of various polymer microchannels, some inherent drawbacks are yet to be solved. For example, the aforementioned approaches inevitably require an additional irreversible sealing process such as plasma oxidation, lamination, UV irradiation, and temperature annealing.[5] In addition, intrinsically hydrophobic PDMS material is often used for the top and/or the bottom layers of the microchannel. While the hydrophobic nature of PDMS can be modified into hydrophilic by utilizing various surface modification techniques such as plasma treatment,[6] polymer grafting,[13] covalent bonding,[14] and adsorption of polyelectrolyte,[15] a permanent modification is still challenging due to aging effects.[16,17] In addition, PDMS suffers from absorption of small molecules (*e.g.*, hydrophobic analytes) and evaporation of water, restricting the widespread use in precise microfluidic experiments such as drug discovery, proteomic analysis, and cell culture applications involving micro- and nanomolar concentrations.[18,19] Therefore, an alternative method for fabricating polymer microchannel that does not require irreversible sealing and surface modification is potentially of great benefit.

Herein, we present a facile fabrication method for generating polymer microfluidic channels by exploiting solvent-assisted direct molding of a PMMA solution.[20–22] In our earlier study, we observed that a vertical capillary motion of PMMA solution into the void spaces of PDMS mold can give birth to hollow structures with an embedded cavity under certain conditions.[21] In particular, the use of a low polymer concentration (<15 wt %) and a controlled amount of dispensed polymer solution, as determined by the volume of mold cavity, played an important role in fabricating hollow structures.[21,22] By utilizing this unique feature, a homogeneous, circular or elliptic PMMA microfluidic channel is fabricated here, without additional irreversible channel sealing and surface modification processes. In this bonding-free channel formation, the cavity diameter is largely determined by the polymer concentration, while the channel size is by the amount of drop-dispensed polymer solution. Therefore, these two parameters are systematically varied so as to construct a structural phase plot for various channel dimensions. To seek potential applications of the molded channels, two experiments are performed: blocking absorption and diffusion of small Rhodamine molecules and constructing artificial capillaries using calf pulmonary artery endothelial cells (CPAEs).

Materials and methods

Preparation of PDMS channel molds and PMMA solutions

The PDMS channel molds were fabricated by casting the precursor (Sylgard 184, Dow Corning) on silicon masters. The

[a]*School of Mechanical and Aerospace Engineering, Seoul National University, Seoul, 151-742, Korea. E-mail: sky4u@snu.ac.kr*
[b]*World Class University (WCU) Program on Multiscale Mechanical Design, Seoul National University, Seoul, 151-742, Korea*
† These two authors contributed equally to this work.

masters were prepared by standard photolithography and deep reactive ion etching (RIE), having protruding feature with the impression of microfluidic channels. Various channels were used, which include (1) straight-line channels with one inlet and one outlet (width: 7 μm, 25 μm, 70 μm, 120 μm, and 150 μm, height: 4 μm, 15 μm, 70 μm, 120 μm, and 100 μm, and length: ~2.5 cm); and (2) Y-shaped channels with two inlets and one outlet (width: 250 μm, height: 100 μm, and length: ~3 cm). To cure the PDMS pre-polymer, a mixture of 10 : 1 silicon elastomer and curing agent was poured on silicon master and baked at 70 °C for 1 h. After complete curing, the PDMS channel replica with features sticking in was peeled from the silicon master. Each inlet/outlet of PDMS channel mold was punched prior to use.

For the molding of microchannel, poly(methyl methacrylate) (PMMA, $M_W = 120\,000$, Sigma, St. Louis, MO) was used due to its useful properties such as hydrophilic nature (water contact angle: ~70°),[23] optical transparency,[24] and chemical/mechanical stability.[25] In the experiment, PMMA solution was prepared with different concentrations in toluene (5–15 wt%). The amount of drop-dispensed polymer solution was carefully adjusted according to the size of PDMS channel mold: 2 μl for 7 μm width and 4 μm height straight-line channel, 5 μl for 25 μm width and 15 μm height straight-line channel, 10 μl for 70 μm width and 70μm height straight-line channel, 15 μl for 120 μm width and 120 μm height straight-line channel, 16 μl for 150 μm width and 100 μm height straight-line channel, and 20 μl for 250 μm width and 100 μm height Y-shaped channel.

Fabrication of PMMA microchannels by solvent-assisted direct molding

The fabrication procedure for generating polymer microchannel by solvent-assisted direct molding can be divided into three steps: mold placement, channel formation, and mold removal. After preparing PDMS channel mold and PMMA solution following the procedure described above, PDMS channel mold was placed on the PMMA solution layer that had been drop-dispensed onto glass substrate. In this step, a plate-type weight (1.25 g cm^{-2}) was loaded on top of the PDMS channel mold and a relatively thick PDMS channel mold (>1 cm) was used for two reasons: (i) to prevent the deformation of PDMS channel mold by swelling and (ii) to ensure conformal contact between the PDMS channel mold and the polymer solution layer. In the second step, a low-viscosity polymer solution rapidly filled into the mold cavity by capillary action and the solvent in polymer solution subsequently absorbed into the solvent-permeable PDMS mold and evaporated into air. At this point, a homogeneous polymer microchannel was generated by the interplay between solvent absorption and mass depletion at the bottom. After complete evaporation of solvent (30 min to 1 h), the PDMS channel mold was carefully removed, leaving behind a solidified, molded PMMA microchannel. After forming the molded microchannel, fluids were introduced by capillarity or a hydraulic pressure drop. In the case of pressure-driven flow, polyethylene tubes (BD, Franklin Lakes, NJ) were connected with pre-defined inlets/outlets of molded microchannel. To enhance the mechanical strength of polymer microchannel, UV-curable poly(urethane acrylate) (PUA, 311RM, Minuta Tech.) was drop-dispensed onto microfluidic assembly and subsequently exposed to UV ($\lambda = 250$–400 nm) for a few minutes (<3 min). Fluids were driven into the molded microchannel using a SP200i syringe pump (World Precision Instruments, Sarasota, FL).

Scanning electron microscopy (SEM)

High-resolution scanning electron microscope (SEM) images were taken using a HITACHI S-4800 microscope (Hitachi, Japan) operating at an accelerating voltage of 5 kV. To avoid charging effects, substrates were sputter-coated with Au to the thickness of 30 nm prior to measurement.

Measurement of advancing contact angle (CA)

The advancing CAs of water on flat PMMA surface was measured by increasing the volume of the drop (captive drop method) with a contact angle analyzer (Drop Shape Analysis System DSA100, Kruss, Germany).

Measurement of absorption and diffusion of Rhodamine B dye

To measure time-course absorption and diffusion of Rhodamine molecules, 100 μM Rhodamine B dye (Sigma, St. Louis, MO) in deionized water was introduced into PMMA and PDMS channels (150 μm width and 100 μm height), respectively. The fluorescent intensity was measured under a fluorescent microscopy (IX 71, Olympus Optical Co. Ltd., Tokyo, Japan) over 5 h time span and the measured values were analyzed using Image-pro plus 5.1 (Olympus Optical Co. Ltd., Tokyo, Japan).

Cell culture

CPAE cell line was purchased from American Type Culture Collection (ATCC). CPAEs were cultured in RPMI 1640 medium (Gibco BRL, Grand Island, NY, USA) containing 2.05 mM L-glutamine, 10% Fetal Bovine Serum (FBS), and 100 U ml^{-1} penicillin-streptomycin. The cells were grown in a humidified 5% CO_2 incubator at 37 °C. Prior to cell seeding, the molded microchannel was coated by 1% gelatin (Sigma, St. Louis, MO) for 1 h. For cell seeding, the CPAE cells that had been harvested at a density of 5×10^5 ml^{-1} were infused through the inlet of microchannel. Then, the microchannel was submerged in sufficient cell culture medium on Petri dish (NUNC, Roskilde, Denmark) and the medium was changed every two days. During the cell culture, flow was not applied into the microchannel to exclude the effect of flow-induced shear stress. The cells were cultured for 7 days.

Cell staining

The cultured CPAEs were stained, after near confluency at 3 days of culture. The cells were washed two times with PBS and fixed with 3.7% paraformaldehyde (Sigma, St. Louis, MO) solution in PBS for 15 min at room temperature. After post-washing, the cells were incubated with blocking and permeabilization solution (1% BSA and 0.3% Triton-X 100 in PBS, Sigma, St. Louis, MO) for 10 min. For the nucleus staining, cells were incubated with DAPI (1 : 3000 in PBS, Sigma, St. Louis, MO) for 3 min and washed with PBS three times. For the filamentous actins (F-actin) staining, cells were incubated with TRITC-phalloidin (1 : 200 in PBS, Sigma, St. Louis, MO) for 30 min and washed with PBS three times. After filling of molded microchannel with

mounting medium (Invitrogen, Carlsbad, CA), the fluorescent images were captured under an inverted fluorescence microscope. Magnified fluorescent images along with cross-sectional front- and side-views were captured under a confocal laser microscope (LSM 510, Carl Zeiss, Jena, Germany).

Cell viability test

Cell viability was determined with a live/dead assay kit (Molecular Probes, Eugene, OR) at 6 days of culture. The CPAEs in molded microchannel were incubated with a solution of 2 mM calcein-AM and 4 mM ethidium homodimer-1 for 30 min. Calcein-AM has green fluorescence to detect live cells while ethidium homodimer-1 has red fluorescence to detect dead cells.

Results and discussion

Fabrication of homogeneous, molded microchannel by solvent-assisted direct molding

Fig. 1A shows a schematic illustration for the fabrication of a PMMA microchannel by solvent-assisted direct molding (see the Materials and methods section for details). In the experiment, a PDMS channel mold that had been punched with inlet/outlet parts was directly placed on a drop-dispensed PMMA solution, resulting in a channel replica with the same configuration with the PDMS channel mold. Due to a large difference in the molding geometry between channel part and inlet/outlet reservoirs, different capillary rises were observed. In the channel part (cross-sectional line along A–A′ in Fig. 1B), the solvent absorption occurs mainly through both sidewalls and ceiling of the PDMS channel mold. At a relatively low concentration (~10 wt %), the polymer solution was driven into the periphery of the PDMS mold and then solidified, resulting in a hollow structure in the form of a circular or elliptical microchannel. In the punched parts (cross-sectional line along B–B′ in Fig. 1C), in contrast, the solvent absorption generally takes place through the sidewalls of PDMS mold only, resulting in a uncapped, hollow structure that can act as an inlet or an outlet of microchannel. It is noted that the current direct molding method can be applied to other polymers having similar affinity to PDMS such as poly(styrene) (PS). It was reported that similar hollow structures were formed when PS polymer was dissolved in toluene under identical conditions.[21] Solvent-free prepolymers such as UV-curable PUA resin, however, rendered completely filled microstructures regardless of the channel geometry, suggesting that the solvent absorption and evaporation plays an important role in the formation of hollow structures.[21]

Fig. 1D shows a representative cross-sectional image of molded microchannel (70 μm width and 70 μm height), demonstrating that the channel is a homogeneous conduit of circular profile. Also, optical images of the original PDMS channel (250 μm width and 100 μm height) (Fig. 1E) and its molded PMMA replica (Fig. 1F) show that the channel dimension has been precisely replicated, except for some thickening of the channel wall by capillary action. Although the molded microchannels were slightly shrunken by thick channel walls as a result of continuous solvent absorption and evaporation, they were

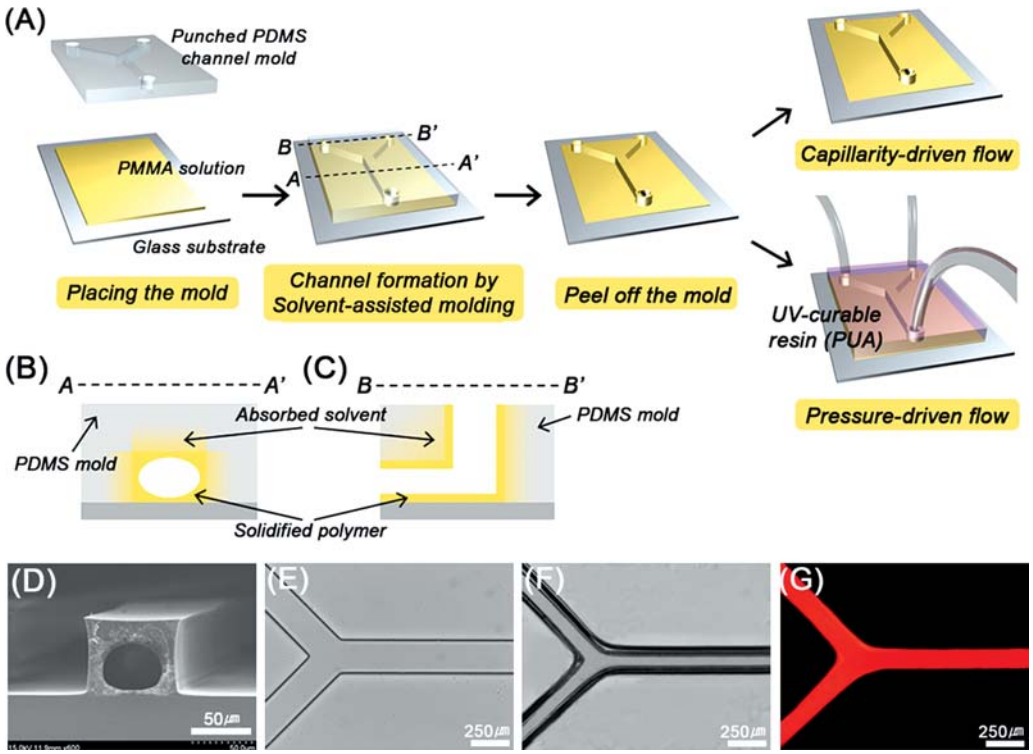

Fig. 1 (A) A schematic illustration for the fabrication of a PMMA microchannel by solvent-assisted direct molding. (B–C) Graphical presentation for the formation of polymer microchannel along the cross-section of (B) A–A′ (channel part) and (C) B–B′ (inlet/outlet parts). (D) Cross-sectional scanning electron microscope (SEM) image of molded microchannel (70 μm width and 70 μm height). (E–G) Inverted optical and fluorescent microscope images of (E) original PDMS channel, (F) its molded microchannel, and (G) liquid flow within the microchannel. For the visualization of liquid flow, a dilute solution of Rhodamine B dye in deionized water was used.

uniformly generated over an extended length over ~3 cm, with good channel definition and physical integrity. The introduction of fluid into the molded microchannel was achieved in two ways: capillary-driven flow and pressure-driven flow. For the use of capillarity, fluid can be directly introduced into a molded microchannel without any additional surface modification, due to the hydrophilic nature (~70°) of PMMA material.[23] Fig. 1G shows such an example of capillary-driven flow of red fluorescent Rhodamine B dye without any leakage. For the pressure-driven flow, UV-curable PUA resin was drop-dispensed onto the microchannel that had been connected with polyethylene tubes and subsequently exposed to UV-irradiation for a few minutes (<3 min). It turned out that PUA could be a suitable material to reinforce the mechanical strength of polymer-based microfluidic systems, owing to its sufficient modulus (~40 MPa) as well as high flexibility.[26]

It is worthwhile noting that the present soft lithographic approach to fabricate a homogeneous, circular microchannel is a simple and low-expertise route compared with other methods. To create a circular microchannel, a number of methods have been proposed, based on thermal reflow,[27] laser melting,[28] and direct writing using femtosecond laser.[29] While these approaches are useful, there are some intrinsic drawbacks that restrict the widespread use of the techniques. For examples, thermal reflow of photoresist or glass is typically conducted with high-temperature and laser melting method also requires high laser fluence. Furthermore, the formation of circular microchannel with uniform cross-sections is not easily achievable in direct writing method. Recently, an alternative method utilizing the meniscus of liquid PDMS in capillary action has been developed.[30] In this approach, a semi-circular or U-shaped PDMS microchannel was fabricated with shape tunable capability and relatively mild experimental conditions. However, this approach also requires an appropriate surface modification and a "double-stacking process" for generating homogeneous, circular feature of microchannel.

Size-controllability of molded microchannel

One of the merits of our approach is the ability to control the dimension of microchannel for a given PDMS channel mold, which can be accomplished by adjusting the initial polymer concentration or the amount of drop-dispensed polymer solution. Fig. 2A shows the variations of channel diameter in molded microchannel as a function of polymer concentration along with the corresponding cross-sectional SEM images. Referring to the inset image, one can define major-axis and minor-axis of elliptic channel as width (W) and height (H), respectively. Then, the variations of both width and height were measured according to the change of polymer concentration (5–11 wt %) by using a straight-line PDMS channel mold (25 μm width, 15 μm height, and 2.5 cm length) under the constant amount of drop-dispensed polymer solution (~5 μl). It is noted here that elliptic microchannel was generated from a PDMS channel mold having a rectangular ($W \neq H$) cross-section, while circular microchannel was fabricated from a PDMS channel mold with square ($W \approx H$) cross-section. As shown in the structural phase plot, both width and height of molded microchannel gradually decreased with inversely proportional to the increase of polymer concentration. This experimental finding demonstrated that the channel diameter in molded microchannel can be tailored from a *single* PDMS channel mold by adjusting the polymer concentration. Interestingly, the rate of decrease in width is slightly larger than that in height. This is presumably because the solvent absorption that determines the mass flow of polymer solution occurred largely through both sidewalls of PDMS mold in horizontal direction as compared to that in vertical direction.

Fig. 2B–G shows cross-sectional SEM images for various molded microchannels with different dimensions. To demonstrate the controllability over the size of microchannel, a broad range of microscale channel dimensions were used with straight-line channels (~2.5 cm length). Here, three different channel widths were used in the decreasing order of 120 μm, 70 μm, and 7 μm with

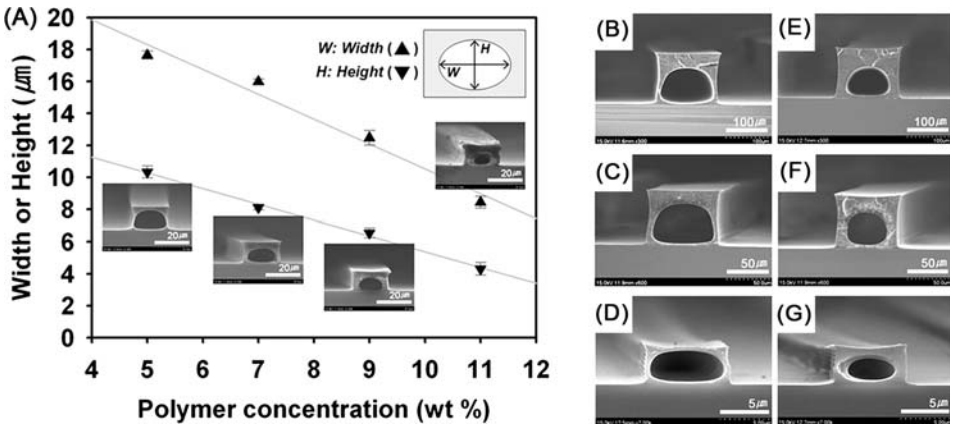

Fig. 2 (A) The variation of channel diameter in molded microchannel as a function of polymer concentration and corresponding cross-sectional SEM images. A straight-line PDMS channel mold (25 μm width and 15 μm height) was used for a constant amount of drop-dispensed polymer solution (~5 μl), with varying polymer concentrations (5–11 wt %). (B–G) Cross-sectional SEM images for various molded microchannels with different dimensions. Under constant polymer concentration (~7 wt %), the amount of drop-dispensed polymer solution was adjusted as follows: (B) 15 μl for 120 μm width, 120 μm height, and 2.5 cm length straight-line channel, (C) 10 μl for 70 μm width, 70 μm height, and 2.5 cm length straight-line channel, and (D) 2 μl for 7 μm width, 4 μm height, and 2.5 cm length straight-line channel. (E–G) Cross-sectional SEM images for molded microchannels using a higher polymer concentration (~10 wt %), while maintaining the other conditions the same with B–D.

the corresponding heights of 120 μm, 70 μm, and 4 μm, respectively. In order to determine an appropriate amount of polymer solution that is needed to form a hollow structure, a set of experiments were carried out with a constant polymer concentration (~7 wt %). As a result, the amount of PMMA solution was roughly adjusted to ~15 μl, 10 μl, and 2 μl for the channels of 120 μm width and 120 μm height (Fig. 2B), 70 μm width and 70 μm height (Fig. 2C), and 7 μm width and 4 μm height (Fig. 2D), respectively. Once an optimal amount of drop-dispensed polymer solution was determined, the channel diameter and shape were further turned by controlling the polymer concentration. Fig. 2E–G shows such an example with the use of a relatively higher polymer concentration (~10 wt %), while maintaining the other conditions the same with Fig. 2B–D. As shown in the figures, the channel diameter was additionally decreased with thicker walls, with the shape being more circular and rounded as compared to that for a lower concentration in Fig. 2B–D.

Despite the flexibility for generating a variety of sizes and shapes of microchannel, it is difficult to fabricate a multiscale channel (*e.g.*, microchannels connected by nanochannels) because the size of molded microchannel is determined by the amount of drop-dispensed polymer solution. To address this shortcoming, a further study would be required to develop an alternative technique such as locally controlled dispensing of polymer solution (*i.e.*, a large amount for microchannel part and a small amount for nanochannel part).

Blocking adsorption and diffusion of Rhodamine B dye

It has been reported that uptake of small molecules by PDMS affects the outcome of microfluidic experiments especially when a very small amount of analyte (micro- and nanomolar concentrations) is involved.[31] Also, hydrophobic analytes can be absorbed in the bulk PDMS or onto its surface, thereby deteriorating separation efficiencies of PDMS channel as compared to glass devices.[32] To overcome some of the limitations, several researchers have attempted to alleviate the absorption of small molecules into PDMS by surface modification including sol–gel techniques[32] and surface coating with a polybrene solution[33] or by adding a surfactant to the working fluid.[34]

The molded PMMA channels presented here offer an alternative to these approaches in a simple and efficient manner. To

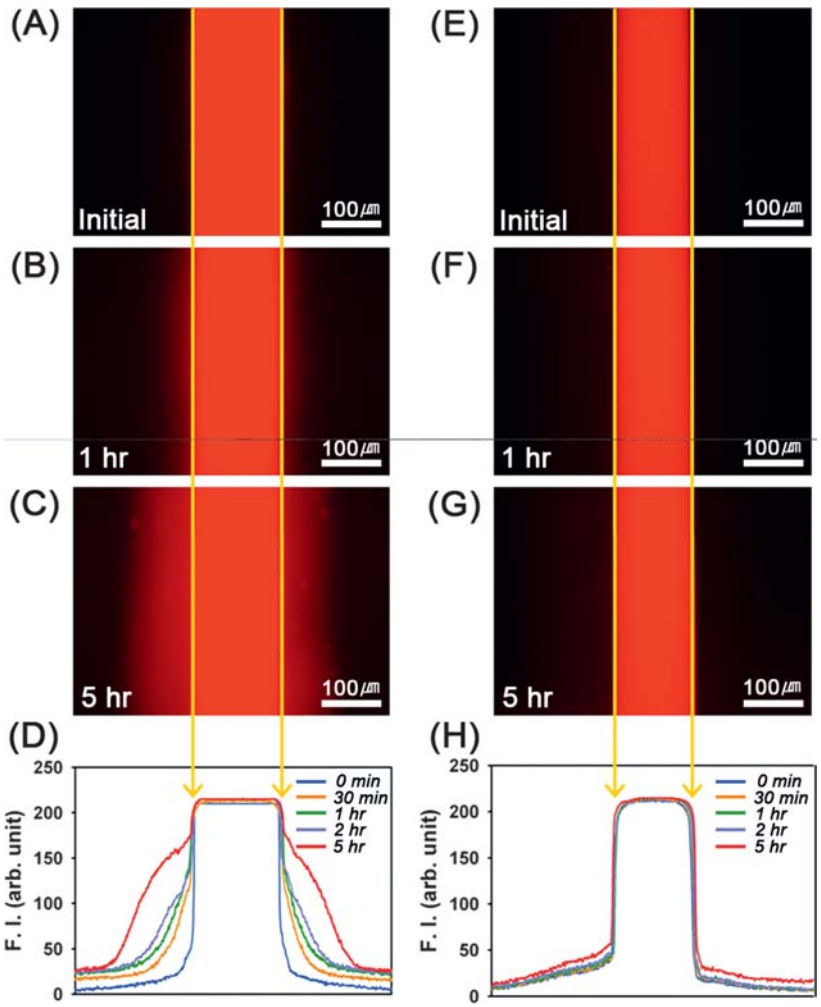

Fig. 3 (A–D) Inverted fluorescent microscope images of red fluorescent Rhodamine B dye inside the PDMS channel at (A) 0 h, (B) 1 h, and (C) 5 h and (D) corresponding fluorescent intensity profiles. (E–F) Inverted fluorescent microscope images of red fluorescent Rhodamine B dye inside the molded PMMA channel at (E) 0 h, (F) 1 h, and (G) 5 h and (H) corresponding fluorescent intensity profiles.

demonstrate the capability of blocking adsorption and diffusion of small molecules, a red fluorescent Rhodamine B dye was introduced into PDMS and PMMA channels (150 μm width and 100 μm height), respectively. The fluorescent intensities were monitored over 5 h time span under a fluorescent microscope. Fig. 3A–C shows a series of fluorescent images over time (0, 1 and 5 h) for the PDMS channel together with plot for the measured fluorescent intensities (Fig. 3D). As can be seen from the figures, a significant amount of the dye is absorbed into PDMS and diffuses with time. In contrast, the molded PMMA channel efficiently blocked the absorption and diffusion of the dye, as supported by the time-course fluorescent images in Fig. 3E–G as well as the overlapped fluorescent profiles with time (Fig. 3H). To evaluate the blocking efficiency for two channels, the fluorescent intensity of diffused dye molecules from the boundary was integrated at each time point and normalized with respect to the initial intensity. The measured ratio was 5.75 for PDMS and 1.12 for PMMA after 5 h of diffusion, respectively, indicating that the blocking efficiency of PMMA channel was about 40 times higher than that of PDMS channel. These results suggest that the molded PMMA channel can be used as an efficient microfluidic platform for blocking adsorption and diffusion of small molecules. Although not shown, the molded channel would also prevent water evaporation for a prolonged period of time since the gas permeability of PMMA is significantly lower than that of PDMS.[35]

Endothelial cell culture inside the molded microchannel

In vascular science, it is important to culture and manipulate cells within a three-dimensional channel network that mimics the *in vivo* vascular architectures.[36,37] In this sense, a circular, homogeneous microfluidic channel presented in this study has the potential to provide useful tools for understanding vascular function and dysfunction, based on the similarity in shape with natural veins as well as the uniformity in the diffusion of nutrition and gases.[30] To demonstrate such capability of molded microchannel as a cell culture platform, calf pulmonary artery endothelial cells (CPAEs) were cultured inside the molded microchannel.

Fig. 4 shows representative results of cultured CPAEs inside the molded microchannel. As seen from the merged nuclei- and F-actins-staining fluorescent image in Fig. 4A, the CPAEs adhered, spread, and proliferated uniformly within the circular PMMA channel to form complete confluency after 3 days of culture. In addition, cell viability was also tested after 6 days of culture to demonstrate biocompatibility and long-term cell culture. As shown in Fig. 4B-C, most cells were stained by calcein-AM (green fluorescence in Fig. 4B), whereas only a few cells were stained by ethidium homodimer-1 (red fluorescence in Fig. 4C), indicating that the viability was larger than 95%.

Several notable findings were derived from the observation of cell adhesion morphology. First, the F-actin bundles of CPAEs highly aligned along the channel direction (Fig. 4D–E), suggesting that the cells are robust and induce an enhanced phenotype of endothelial cells. It was reported that cells can recognize a surface curvature and thus the cell adhesion is decreased on a concave surface as compared with a convex or a flat surface.[38] In our system, the molded microchannel has a concave curvature around the periphery (red arrow in Fig. 4F), whereas a relatively flat mesa

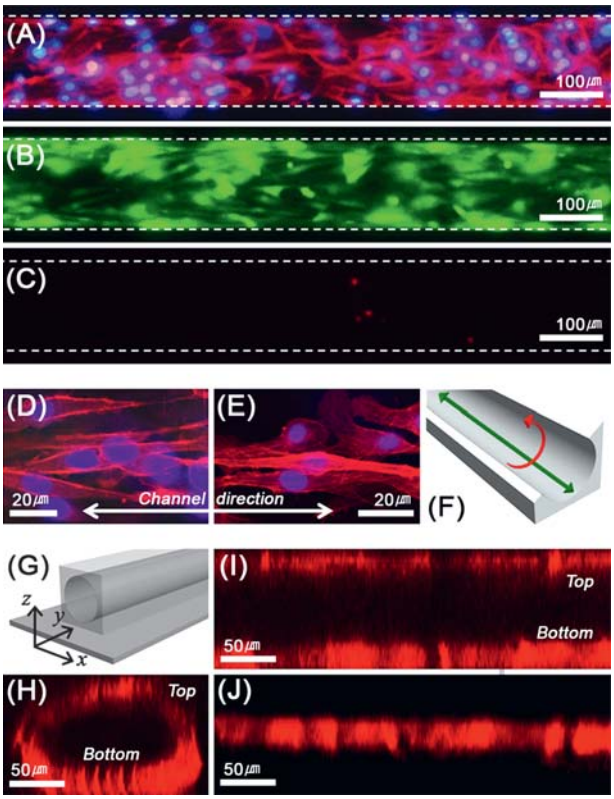

Fig. 4 (A) An inverted fluorescent microscope image for cultured CPAEs within the molded microchannel after 3 days of culture. Red (filamentous actins-staining) and blue (nuclei-staining) fluorescent images were obtained and merged. (B–C) Cell viability test after 6 days of culture. The live-cells were stained by calcein-AM (green), whereas dead-cells were stained by ethidium homodimer-1 (red). The viability was higher than 95%. (D–E) Magnified fluorescent confocal laser microscope images of CPAEs, stained for F-actins and nuclei. The CPAEs highly aligned along the channel direction. (F) Graphical presentation for the geometric characteristic of molded microchannel. The molded microchannel has a concave curvature around the periphery (red arrow) and a relatively flat mesa along the longitudinal direction (green arrow). (G) Graphical presentation of molded microchannel with three-dimensional (3D) coordination. Cross-sectional front-view was obtained along the *zx*-plane and side-views were obtained along the *yz*-plane. (H–J) Fluorescent cross-sectional views of the cells, stained for F-actin. Cross-sectional front-view (H), side-view for top and bottom (I), and side-view for lateral side (J) were obtained by confocal laser microscope.

is seen along the longitudinal direction (green arrow in Fig. 4F). Owing to this geometric characteristic, the cells tended to align along the channel direction, without any shear flow or an external surface texture such as micro- or nanoscale patterns.[39,40] Second, the cells spread uniformly within the channel and formed a 3D architecture as seen from the fluorescent images in Fig. 4H–J. Using confocal laser microscopy, various cross sectional fluorescent images of F-actin were taken in different directions including front-view (Fig. 4H, cross-section along the *zx*-plane in Fig. 4G), side-view for top and bottom (Fig. 4I, cross-section along the *yz*-plane n Fig. 4G), and side-view for lateral side (Fig. 4J, cross-section along the *yz*-plane in Fig. 4G). As shown, the CPAEs covered the whole channel with relatively uniform distribution. It was observed that the cells adhered on the bottom of microchannel in a larger number as compared to the top and lateral

sides. Such an enhanced cell adhesion appears to be associated with many contributions including cell sedimentation and a relatively flat mesa on the channel bottom. The homogeneous, circular PMMA microchannel presented here can guide the adhesion and aligned growth of endothelial cells with a three-dimensional architecture, allowing for a useful tool for *in vitro* experimentation of artificial cell-cultured capillaries.

Conclusions

We have presented a direct molding method for creating a homogenous, circular or elliptic microfluidic channel by utilizing solvent-assisted molding technique. Our soft lithographic approach would be useful in several aspects. First, a polymer microchannel can be fabricated without any additional channel sealing and surface modification processes. Second, the dimension of molded microchannel can be tuned by adjusting the initial polymer concentration and the amount of polymer solution for a given PDMS mold geometry. It was found that the channel diameter in molded microchannel was varied inversely proportional to the polymer concentration. Furthermore, an extended microchannel of ~3 cm was generated by controlling the amount of drop-dispensed polymer solution without clogging or significant size variation. Third, the introduction of aqueous solution into the molded microchannel was achieved in the form of either capillarity-driven or pressure-driven flow.

The homogeneous, circular molded microchannel is also advantageous for several potential applications such in blocking absorption and diffusion of small molecules and in constructing artificial endothelial cell-cultured capillaries. With the use of red fluorescent Rhodamine B dye, the blocking performance of PMMA microchannel was evaluated and compared with PDMS channel. It turned out that the absorption and diffusion can be efficiently prevented in PMMA channel with its efficiency approximately 40 times larger than that of porous PDMS channel. Also, it was observed that the CPAEs adhered, spread, and proliferated to near confluency within 3 days and remained viable up to 6 days with *in vivo*-like three-dimensional structure, demonstrating good biocompatibility as well as long-term cell culture capability for constructing artificial endothelial cell-cultured capillaries.

Acknowledgements

This work was supported by the WCU (World Class University) program (R31-2008-000-10083-0) and Basic Science Research Program (2010-0027955) through the Korea Science and Engineering Foundation grant funded by the Ministry of Education, Science and Technology (MEST). This work was supported in part by the Center for Nanoscale Mechatronics & Manufacturing (08K1401-00710), one of the 21st Century Frontier Research Programs in Korea. We also thank Duck-Gyu Lee for operating high-speed camera.

References

1 D. J. Beebe, G. A. Mensing and G. M. Walker, *Annu. Rev. Biomed. Eng.*, 2002, **4**, 261–286.
2 S. M. Kim, S. H. Lee and K. Y. Suh, *Lab Chip*, 2008, **8**, 1015–1023.
3 P. Kim, K. W. Kwon, M. C. Park, S. H. Lee, S. M. Kim and K. Y. Suh, *Biochip J.*, 2008, **2**, 1–11.
4 E. Delamarche, D. Juncker and H. Schmid, *Adv. Mater.*, 2005, **17**, 2911–2933.
5 J. Rossier, F. Reymond and P. E. Michel, *Electrophoresis*, 2002, **23**, 858–867.
6 D. C. Duffy, J. C. McDonald, O. J. A. Schueller and G. M. Whitesides, *Anal. Chem.*, 1998, **70**, 4974–4984.
7 D. J. Beebe, J. S. Moore, Q. Yu, R. H. Liu, M. L. Kraft, B. H. Jo and C. Devadoss, *Proc. Natl. Acad. Sci. U. S. A.*, 2000, **97**, 13488–13493.
8 X. Liu, Q. Wang, J. H. Qin and B. C. Lin, *Lab Chip*, 2009, **9**, 1200–1205.
9 D. Huh, K. L. Mills, X. Y. Zhu, M. A. Burns, M. D. Thouless and S. Takayama, *Nat. Mater.*, 2007, **6**, 424–428.
10 S. Chung, J. H. Lee, M. W. Moon, J. Han and R. D. Kamm, *Adv. Mater.*, 2008, **20**, 3011–3016.
11 D. Wright, B. Rajalingam, S. Selvarasah, M. R. Dokmeci and A. Khademhosseini, *Lab Chip*, 2007, **7**, 1272–1279.
12 P. Kim, H. E. Jeong, A. Khademhosseini and K. Y. Suh, *Lab Chip*, 2006, **6**, 1432–1437.
13 S. W. Hu, X. Q. Ren, M. Bachman, C. E. Sims, G. P. Li and N. Allbritton, *Anal. Chem.*, 2002, **74**, 4117–4123.
14 J. H. Zhou, H. Yan, K. N. Ren, W. Dai and H. K. Wu, *Anal. Chem.*, 2009, **81**, 6627–6632.
15 S. L. R. Barker, M. J. Tarlov, H. Canavan, J. J. Hickman and L. E. Locascio, *Anal. Chem.*, 2000, **72**, 4899–4903.
16 H. Makamba, J. H. Kim, K. Lim, N. Park and J. H. Hahn, *Electrophoresis*, 2003, **24**, 3607–3619.
17 C. S. Chen, D. N. Breslauer, J. I. Luna, A. Grimes, W. C. Chin, L. P. Leeb and M. Khine, *Lab Chip*, 2008, **8**, 622–624.
18 M. W. Toepke and D. J. Beebe, *Lab Chip*, 2006, **6**, 1484–1486.
19 A. R. Abate, D. Lee, T. Do, C. Holtze and D. A. Weitz, *Lab Chip*, 2008, **8**, 516–518.
20 K. Y. Suh, M. C. Park and P. Kim, *Adv. Funct. Mater.*, 2009, **19**, 2699–2712.
21 S. H. Lee, H. N. Kim, R. K. Kwak and K. Y. Suh, *Langmuir*, 2009, **25**, 12024–12029.
22 S. H. Lee, H. E. Jeong, M. C. Park, J. Y. Hur, H. S. Cho, S. H. Park and K. Y. Suh, *Adv. Mater.*, 2008, **20**, 788–792.
23 L. Martynova, L. E. Locascio, M. Gaitan, G. W. Kramer, R. G. Christensen and W. A. MacCrehan, *Anal. Chem.*, 1997, **69**, 4783–4789.
24 W. H. Zhang, S. C. Lin, C. M. Wang, J. Hu, C. Li, Z. X. Zhuang, Y. L. Zhou, R. A. Mathies and C. Y. J. Yang, *Lab Chip*, 2009, **9**, 3088–3094.
25 A. Muck, J. Wang, M. Jacobs, G. Chen, M. P. Chatrathi, V. Jurka, Z. Vyborny, S. D. Spillman, G. Sridharan and M. J. Schoning, *Anal. Chem.*, 2004, **76**, 2290–2297.
26 S. J. Choi, P. J. Yoo, S. J. Baek, T. W. Kim and H. H. Lee, *J. Am. Chem. Soc.*, 2004, **126**, 7744–7745.
27 G. J. Wang, C. C. Hsueh, S. H. Hsu and H. S. Hung, *J. Micromech. Microeng.*, 2007, **17**, 2000–2005.
28 Q. F. Xia, K. J. Morton, R. H. Austin and S. Y. Chou, *Nano Lett.*, 2008, **8**, 3830–3833.
29 F. He, Y. Cheng, Z. Z. Xu, Y. Liao, J. Xu, H. Y. Sun, C. Wang, Z. H. Zhou, K. Sugioka, K. Midorikawa, Y. H. Xu and X. F. Chen, *Opt. Lett.*, 2010, **35**, 282–284.
30 K. Lee, C. Kim, K. S. Shin, J. Lee, B. K. Ju, T. S. Kim, S. K. Lee and J. Y. Kang, *J. Micromech. Microeng.*, 2007, **17**, 1533–1541.
31 G. T. Roman, K. McDaniel and C. T. Culbertson, *Analyst*, 2006, **131**, 194–201.
32 G. T. Roman, T. Hlaus, K. J. Bass, T. G. Seelhammer and C. T. Culbertson, *Anal. Chem.*, 2005, **77**, 1414–1422.
33 R. Samy, T. Glawdel and C. L. Ren, *Anal. Chem.*, 2008, **80**, 369–375.
34 Y. H. Xu, H. Jiang and E. K. Wang, *Electrophoresis*, 2007, **28**, 4597–4605.
35 J. E. Mark, *Polymer Data Handbook*, Oxford University Press, New York, 1999.
36 J. B. Shao, L. Wu, J. Z. Wu, Y. H. Zheng, H. Zhao, Q. H. Jin and J. L. Zhao, *Lab Chip*, 2009, **9**, 3118–3125.
37 V. Vickerman, J. Blundo, S. Chung and R. Kamm, *Lab Chip*, 2008, **8**, 1468–1477.
38 V. Vogel and M. Sheetz, *Nat. Rev. Mol. Cell Biol.*, 2006, **7**, 265–275.
39 S. Y. Hwang, K. W. Kwon, K. J. Jang, M. C. Park, J. S. Lee and K. Y. Suh, *Anal. Chem.*, 2010, **82**, 3016–3022.
40 D. H. Kim, E. A. Lipke, P. Kim, R. Cheong, S. Thompson, M. Delannoy, K. Y. Suh, L. Tung and A. Levchenko, *Proc. Natl. Acad. Sci. U. S. A.*, 2010, **107**, 565–570.

